



Original research

Diagnostic confidence with quantitative cardiovascular magnetic resonance perfusion mapping increases with increased coverage of the left ventricle

Henrik Engblom^{a,*}, Ellen Ostenfeld^a, Marcus Carlsson^a, Julius Åkesson^a, Anthony H. Aletras^{a,b}, Hui Xue^c, Peter Kellman^c, Håkan Arheden^a

^a Clinical Physiology, Department of Clinical Sciences Lund, Lund University, Skåne University Hospital, Lund, Sweden

^b Laboratory of Computing, Medical Informatics and Biomedical-Imaging Technologies, School of Medicine, Aristotle University of Thessaloniki, Thessaloniki, Greece

^c National Heart-Lung and Blood Institute, National Institutes of Health, Bethesda, MD, USA

ARTICLE INFO

Keywords:

Myocardial perfusion
Coronary artery disease
Diagnostic confidence
Cardiovascular magnetic resonance
Quantitative first-pass perfusion

ABSTRACT

Background: Quantitative cardiovascular magnetic resonance (CMR) first pass perfusion maps are conventionally acquired with 3 short-axis (SAX) views (basal, mid, and apical) in every heartbeat (3SAX/1RR). Thus, a significant part of the left ventricle (LV) myocardium, including the apex, is not covered. The aims of this study were 1) to investigate if perfusion maps acquired with 3 short-axis views sampled every other RR-interval (2RR) yield comparable quantitative measures of myocardial perfusion (MP) as 1RR and 2) to assess if acquiring 3 additional perfusion views (i.e., total of 6) every other RR-interval (2RR) increases diagnostic confidence.

Methods: In 287 patients with suspected ischemic heart disease stress and rest MP were performed on clinical indication on a 1.5T MR scanner. Eighty-three patients were examined by acquiring 3 short-axis perfusion maps with 1RR sampling (3SAX/1RR); for which also 2RR maps were reconstructed. Additionally, in 103 patients 3 short-axis and 3 long-axis (LAX; 2-, 3, and 4-chamber view) perfusion maps were acquired using 2RR sampling (3SAX + 3LAX/2RR) and in 101 patients 6 short-axis perfusion maps using 2RR sampling (6SAX/2RR) were acquired. The diagnostic confidence for ruling in or out stress-induced ischemia was scored according to a Likert scale (certain ischemia [2 points], probably ischemia [1 point], uncertain [0 points], probably no ischemia [1 point], certain no ischemia [2 points]).

Results: There was a strong correlation ($R = 0.99$) between 3SAX/1RR and 3SAX/2RR for global MP (mL/min/g). The diagnostic confidence score increased significantly when the number of perfusion views was increased from 3 to 6 (1.24 ± 0.68 vs 1.54 ± 0.64 , $p < 0.001$ with similar increase for 3SAX+3LAX/2RR (1.29 ± 0.68 vs 1.55 ± 0.65 , $p < 0.001$) and for 6SAX/2RR (1.19 ± 0.69 vs 1.53 ± 0.63 , $p < 0.001$).

Conclusion: Quantitative perfusion mapping with 2RR sampling of data yields comparable perfusion values as 1RR sampling, allowing for the acquisition of additional views within the same perfusion scan. The diagnostic confidence for stress-induced ischemia increases when adding 3 additional views, short- or long axes, to the conventional 3 short-axis views. Thus, future development and clinical implementation of quantitative CMR perfusion should aim at increasing the LV coverage from the current standard using 3 short-axis views.

1. Introduction

Coronary artery disease (CAD) is one of the major causes of death worldwide and is characterized by flow limiting obstructions of the

coronary arteries affecting myocardial perfusion [1]. In the situation of suspected CAD, cardiovascular magnetic resonance (CMR) imaging can be used to evaluate myocardial perfusion using dynamic first-pass perfusion (FPP) imaging at rest and during vasodilator stress [2,3]. In

Abbreviations: CMR, cardiovascular magnetic resonance; SAX, short axis; LV, left ventricle; MP, myocardial perfusion; LAX, long axis; CAD, coronary artery disease; FPP, first pass perfusion; qFPP, quantitative first pass perfusion; AHA, American Heart Association; PET, positron emission tomography; MVD, microvascular dysfunction; SSFP, steady state free precession; AIF, arterial input function; LCX, left circumflex coronary artery; RCA, right coronary artery; LAD, left anterior descending coronary artery; ACEinh, angiotensin converting enzyme inhibitor; ARB, angiotensin receptor blocker; CABG, coronary artery bypass grafting; BPM, beats per minute; EPI, echo planar imaging; SPECT, single photon emission computed tomography

* Corresponding author. Department of Clinical physiology, Skåne University Hospital, SE-221 85 Lund, Sweden.

E-mail address: henrik.engblom@med.lu.se (H. Engblom).

<https://doi.org/10.1016/j.jocmr.2024.101007>

Received 10 November 2023; Received in revised form 14 January 2024; Accepted 30 January 2024

1097-6647/© 2024 The Authors. Published by Elsevier Inc. on behalf of Society for Cardiovascular Magnetic Resonance. This is an open access article under the CC BY-NC-ND license (<http://creativecommons.org/licenses/by-nc-nd/4.0/>).

FPP, a series of dynamic single-shot images are acquired as an intravenously injected bolus of a gadolinium-based contrast agent is entering the heart and passing through the myocardium. Conventional FPP has traditionally been evaluated and interpreted based on qualitative [2,4] or semi-quantitative [5,6] assessment of myocardial perfusion for detection of myocardial ischemia. Quantitative perfusion has shown clinical value both regarding increased diagnostic accuracy of coronary stenosis [7] and prognostic outcome [8]. Furthermore, the current American Heart Association (AHA) guidelines recommend quantitative perfusion with positron emission tomography (PET) or CMR to detect microvascular dysfunction (MVD) in patients with ischemia and non-obstructive coronary angiography [9].

The underlying theoretical framework for quantitative perfusion imaging was presented already in the early 1960s [10] and was first applied by Leon Axel in dynamic cardiac computed tomography [11]. Fully quantitative FPP (qFPP) has since then been introduced, enabling pixelwise myocardial perfusion quantification in mL/min/g using either dual-bolus techniques [12,13] or a dual sequence, single bolus approach [14–16]. FPP images are commonly acquired in 3 short-axis slices (basal, middle, and apical) of the left ventricle (LV), with single-shot acquisition of each slice every RR-interval (1RR). This approach allows for assessment of myocardial perfusion in 16 of the 17 LV segments recommended for regional myocardial distribution of perfusion [17]. Still, a significant part of the myocardium is not covered with only 3 short-axis 8 mm slices and regional inhomogeneities in perfusion can be missed. This is a limitation when compared to cardiac nuclear imaging, such as PET with full 3-dimensional LV coverage for perfusion assessment [18,19]. In other words, while in-plane resolution with FPP CMR is high compared to nuclear imaging, typically 2×2 mm versus 6×6 mm, the contrary is true throughout the long-axis plane of the LV where nuclear imaging has the same resolution but the convention in CMR uses only 3 slices (basal, mid, and apical). Increased coverage of the LV, including long-axis imaging, would potentially increase the diagnostic confidence when interpreting qFPP images, e.g., by improved coverage of the base and LV apex.

The LV coverage using qFPP can be increased by increasing the number of slices acquired during the bolus injection. However, more slices require increased acquisition time, usually not possible to fit in a single RR-interval (1RR), especially during stress when the heart rate increases. A solution to this problem would be to acquire 2 sets of images with perfusion sampling every other RR interval (2RR) for each set of images. To what extent sampling perfusion data every 2RR intervals is sufficient for maintaining accurate assessment of quantitative perfusion has not been described in the literature.

The aims of this study were 1) to determine if a 2RR versus a 1RR sampling interval for dual sequence, single bolus qFPP affects the quantitative perfusion values and 2) to assess if adding 3 long-axis slices (2-, 3-, and 4-chamber views) or 3 short-axis slices, in addition to the conventional 3 short-axis slices, increases the diagnostic confidence with this qFPP technique.

2. Methods

2.1. Study population

A total of 287 patients referred for stress CMR to the Department of Clinical Physiology and the Skåne University Hospital, Lund, Sweden, due to suspected chronic coronary syndrome were prospectively included in the study (November 2020–September 2021). All patients were examined by CMR with qFPP using single bolus, dual sequence perfusion mapping for assessment of myocardial perfusion to confirm or rule out stress-induced myocardial ischemia [14,15]. Eighty-three consecutive clinical patients were examined by acquiring 3 short-axis (SAX) perfusion maps with 1RR sampling (February–March 2021), 101 consecutive patients by acquiring 6 SAX perfusion maps using 2RR sampling (November 2020–February 2021) and 103 consecutive

patients by acquiring 3 SAX and 3 long-axis (LAX) (2-, 3-, and 4-chamber) perfusion maps using 2RR sampling (June–September 2021). Inclusion criteria were sinus rhythm, age > 18 years, the use of adenosine as the pharmacological stressor, and acquisition of both stress and rest perfusion images. Exclusion criteria were contraindication for CMR (estimated glomerular filtration rate < 30 mL/min/1.73 m², ferrometal and device implant, and known contrast agent intolerance). The study was approved by the regional ethics committee and all patients gave their written informed consent to participate in the study.

2.2. Image acquisition and reconstruction

The CMR examinations were performed on either of two 1.5T MR scanners (Siemens Magnetom Sola Cardiovascular Edition or Siemens Magnetom Aera, Siemens Healthineers, Erlangen, Germany). After initial scout imaging to define the short- and long-axis LV image planes, cine steady state free precession (SSFP) SAX images were acquired covering the entire LV (slice thickness 8 mm, no gap). Cine SSFP images were also acquired in the 3, standard LAX planes (2-, 3-, and 4-chamber views, slice thickness 8 mm).

For each patient qFPP images were acquired both during adenosine stress after 3 min of intravenous adenosine infusion (140–210 µg/kg/min) and approximately 10 min later at rest. For both stress and rest imaging, an intravenous injection of 0.05 mmol/kg gadolinium (Gd)-based contrast agent (Clariscan – gadoterate meglumine, GE Healthcare, Danderyd, Sweden) was administered as previously described [15]. In short, single-shot images using a single bolus, dual sequence strategy where low-resolution images for arterial input function (AIF) and high-resolution images for myocardial perfusion are acquired simultaneously. The images are reconstructed automatically, generating a pixelwise map where the perfusion is displayed online at the scanner in colors directly corresponding to specific numbers of absolute perfusion in mL/min/g. A convolution neural net approach was used to automatically segment the perfusion map into the AHA LV segment model as previously described [20] also performed online. The online image reconstruction and generation of perfusion maps is performed within 90 s.

2.2.1. 1RR sampling, 3 SAX views (n = 83)

For sampling every heartbeat (1RR), qFPP myocardial images were acquired in 3 SAX views (basal, mid, and apical) during 60 heartbeats both during adenosine stress and at rest. The AIF images were acquired for the basal SAX slice sampled every heartbeat (1RR) using the dual sequence.

2.2.2. 2RR sampling, 3SAX + 3LAX or 6 SAX views (n = 204)

For every other heartbeat (2RR) sampling, qFPP myocardial images were acquired either in A) 3SAX (basal, mid, and apical) + 3LAX (2-, 3- and 4-chamber view; Fig. 1A) or B) 6 SAX views equally distributed from base to apex (Fig. 1B). The qFPP acquisition in the 6 image views was performed during 120 heartbeats at stress and rest. In both cases, the AIF images were acquired for the basal SAX slice sampled every heartbeat (1RR) using the dual sequence.

2.3. MR image analysis

2.3.1. 1RR vs 2RR for quantitative perfusion (n = 83)

To allow for direct comparison of quantitative perfusion between 1RR and 2RR sampling of the myocardial images, stress and rest perfusion maps from the 83 patients with 1RR sampling were computed using data both from 1RR and from 2RR by discarding alternate heartbeats. Global and regional (according to the 17-segment model [17]) perfusion were derived from both 1RR and 2RR sampling perfusion maps and expressed as mL/min/g myocardial tissue.

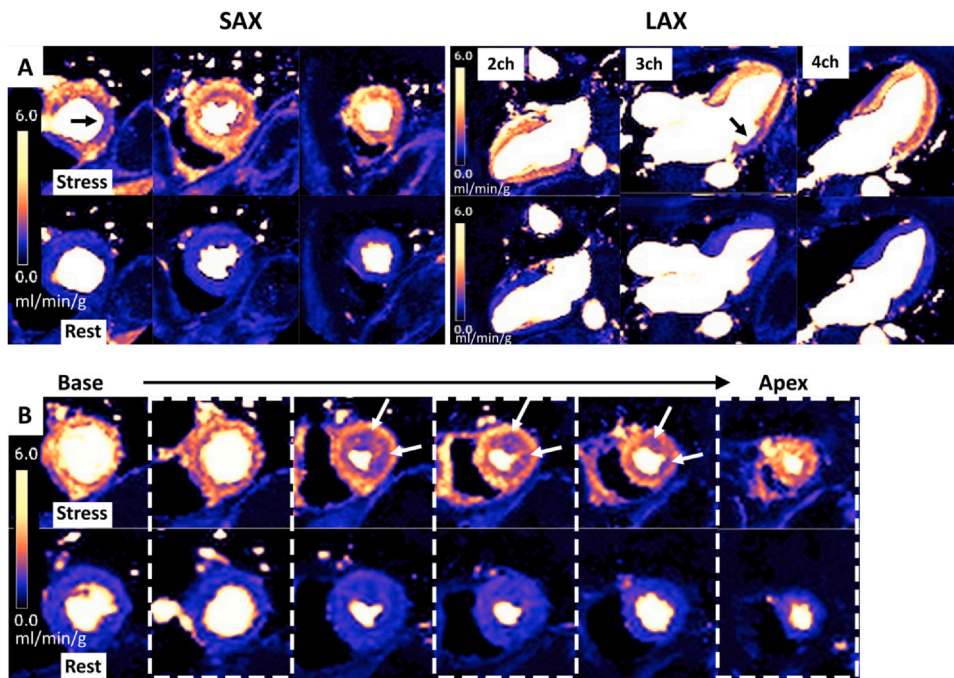


Fig. 1. Perfusion maps from 2 patients with 6 views acquired with 2RR sampling. **A)** A patient with 3SAX + 3LAX (2-, 3-, and 4-chamber) views during adenosine stress (upper panel) and at rest (lower panel). The diagnostic confidence increased when the stress-induced perfusion defect was found in 2 orthogonal planes within the LCX perfusion territory (black arrows in basal SAX and in the 3ch-LAX). **B)** A patient with 6 SAX views during adenosine stress (upper panel) and at rest (lower panel). The 3 conventional SAX views are indicated within the dashed boxes. The diagnostic confidence increased when the stress-induced perfusion defect within the LCX perfusion territory was found in 3 consecutive SAX views (white arrows) instead of only one for the conventional views. 2ch: 2-chamber view, 3ch: 3-chamber view, 4ch: 4-chamber view, LAX: long-axis view, LCX: left circumflex coronary artery, SAX: short-axis view.

2.3.2. 3 vs 6 slices for assessment of ischemia (n = 204)

To test if 6 slices (either 3SAX + 3LAX/2RR or 6SAX/2RR) instead of the conventional 3SAX/2RR views increase the diagnostic confidence when examining patients with qFPP CMR, one observer (H.E., 20+ years of CMR experience) did the analysis of the 204 patients with 2RR sampling. For intra- and interobserver variability, a subset of 40 patients (20 with 3SAX + 3LAX and 20 with 6SAX) were analyzed by the same observer > 1 month apart and by an additional observer (E.O., 17 years of CMR experience). Before performing the interobserver reading, the 2 observers discussed a subset of patients (n = 20) not included in the analysis, to agree on how different findings should be reported. For each patient, 2 sets of perfusion maps were created, one with all 6 slices (3SAX + 3LAX/2RR or 6SAX/2RR) and one with only the 3 SAX slice positions (3SAX/2RR) usually acquired in clinical routine (base, mid, and apical). Each case was evaluated for stress-induced ischemia present/absent, ischemic burden (< 50% or > 50% transmural extent of ischemia for of the LV segments) and in which of the 3 main coronary territories (left anterior descending coronary artery [LAD], left circumflex coronary artery [LCX], and right coronary artery [RCA]) if present. The 3- and 6-view datasets for each patient were blinded and randomly presented to the observers to avoid bias. For each of the data sets, level of confidence according to a 5-grade Likert scale with an associated diagnostic confidence score (0–2 points) as follows: 1 = certain ischemia (2 points), 2 = probably ischemia (1 point), 3 = uncertain (0 points), 4 = probably no ischemia (1 point), and 5 = certain no ischemia (2 points). The observers had access to the motion-corrected and non-motion corrected FPP single-shot images corresponding to the perfusion maps. In addition, the observers had access to automatically generated ECG-signal images, respiratory motion diagrams and RR-interval diagrams to assess potential influence of heavy respiration or arrhythmia/triggering problems on image quality (Supplemental Fig. 1). In addition, sign of splenic switch-off was evaluated in the FPP images for assessment of adenosine effect [21]. In short, splenic switch-off was visually assessed as reduced perfusion of the spleen during adenosine stress imaging compared to rest imaging (spleen being dark in the former and bright in the latter). The observers were blinded to all other imaging data and patient history.

To enable comparison of quantitative perfusion values between SAX and LAX perfusion maps, regions of interest were drawn in the same 20 patients from intra/interobserver analysis (3SAX + 3LAX/2RR) at the 18 intersects between SAX (basal, mid, apical) and LAX (2-, 3-, 4-

chamber view). Intersections with artifacts or outside of the LV myocardium such as the LV outflow tract were excluded. In total, 641 intersections were included in the analysis.

2.4. Invasive coronary angiography

Of the 204 patients included for the 3 vs 6 slice comparison, 50 were clinically referred for invasive angiography within 6 months of the CMR examination. Presence of coronary stenosis for each of the 3 main coronary vessel territories was assessed by the clinical angiographer blinded to the CMR data. The angiography findings were then compared with myocardial perfusion by qFPP in the corresponding vessel territory.

2.5. Statistical analysis

Values are expressed as mean \pm SD unless other is specified. For comparison of quantitative perfusion values between 1RR and 2RR qFPP sampling as well as SAX vs LAX perfusion values, Pearson's correlation and Bland-Altman analysis were performed. Difference in diagnostic confidence score between 3- and 6-views perfusion analysis was assessed by Wilcoxon rank sum test. A p-value < 0.05 was considered to indicate statistical significance.

3. Results

The patients' characteristics are shown in Table 1. The average age was 66 years with 43% (122/287) females. Seventeen percent (48/287) of the patients had known CAD, 13% (38/287) had diabetes and approximately one-third (31%, 90/287) had hypertension.

3.1. Quantitative perfusion with 1RR vs 2RR interval sampling

The first-pass-perfusion curves for 1RR and 2RR interval sampling were similar (Fig. 2). There was an excellent agreement between myocardial perfusion values derived from 1RR interval and 2RR interval sampling both for global perfusion in 160 examinations (83 stress and 77 rest perfusion scans) (bias 0.13 ± 0.08 mL/min/g, $R = 0.99$, $p < 0.001$; Fig. 3A and B) and regional perfusion in 2560 LV segments (bias 0.01 ± 0.34 mL/min/g, $R = 0.95$, $p < 0.001$; Fig. 3C and D).

Table 1
Patient characteristics.

	All (n = 287)	3 SAX (n = 83)	3 SAX + 3 LAX (n = 103)	6 SAX (n = 101)
Age (range)	66 (18–88)	67 (30–88)	66 (18–88)	65 (27–85)
Sex (females)	122 (43%)	40 (48%)	41 (40%)	43 (43%)
Smoker	25 (9%)	9 (11%)	6 (6%)	10 (10%)
Current	10 (3%)	4 (5%)	1 (1%)	5 (5%)
Former	15 (5%)	5 (6%)	5 (5%)	5 (5%)
Diabetes	38 (13%)	8 (10%)	17 (17%)	13 (13%)
Hypertension	90 (31%)	25 (30%)	35 (34%)	30 (30%)
Known CAD	48 (17%)	16 (19%)	14 (14%)	18 (18%)
Prior PCI	45 (16%)	13 (16%)	15 (15%)	17 (17%)
Prior CABG	19 (7%)	2 (2%)	5 (5%)	12 (12%)
Statins	103 (36%)	30 (36%)	30 (29%)	43 (43%)
ACE-inh/ARB	97 (34%)	25 (30%)	31 (30%)	41 (41%)
Anticoagulants	118 (41%)	38 (46%)	36 (35%)	44 (44%)

Data expressed as median and range or absolute numbers and proportion.

ACE-inh angiotension-converting enzyme inhibitor, ARB angiotensin II receptor blockers, CABG coronary artery bypass grafting, CAD coronary artery disease, LAX long-axis views, PCI percutaneous coronary intervention, SAX short-axis views.

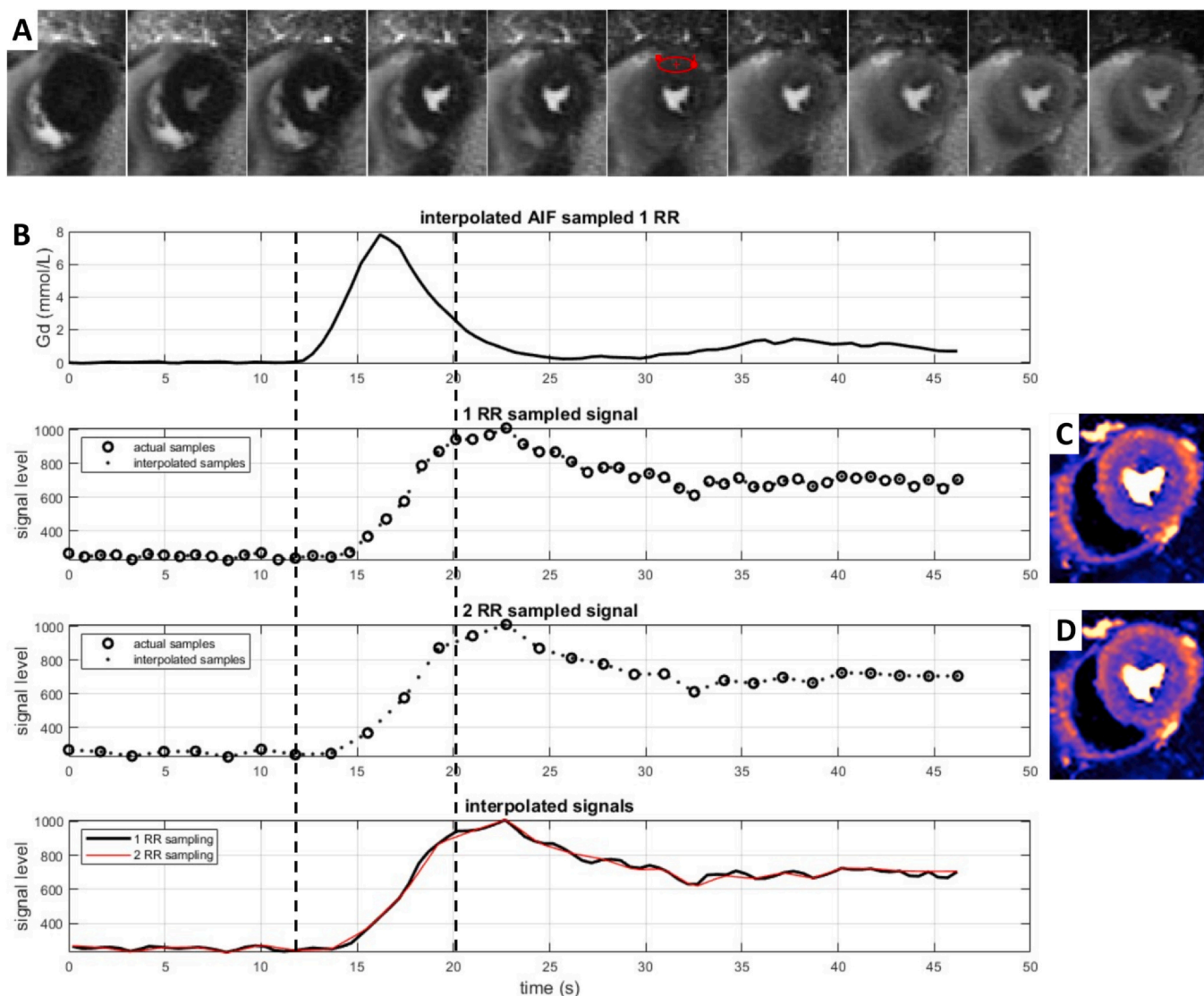


Fig. 2. First-pass perfusion images (A), AIF and time-intensity curves (B) as well as resulting perfusion maps for 1RR and 2RR interval sampling in the same patient (C, D). The red region of interest represents the myocardium from which the myocardial time-intensity curves were generated. The dashed horizontal lines indicate the times between which the first-pass perfusion images in (A) were acquired. Note that the 2RR-sampled curve is a downsampling of the 1RR acquisition resulting in similar time-intensity curves (B, lower panel). Note the similarity between the resulting quantitative perfusion maps (C, D). 1RR: sampling every RR-interval, 2RR: sampling every other RR-interval, AIF: arterial input function.

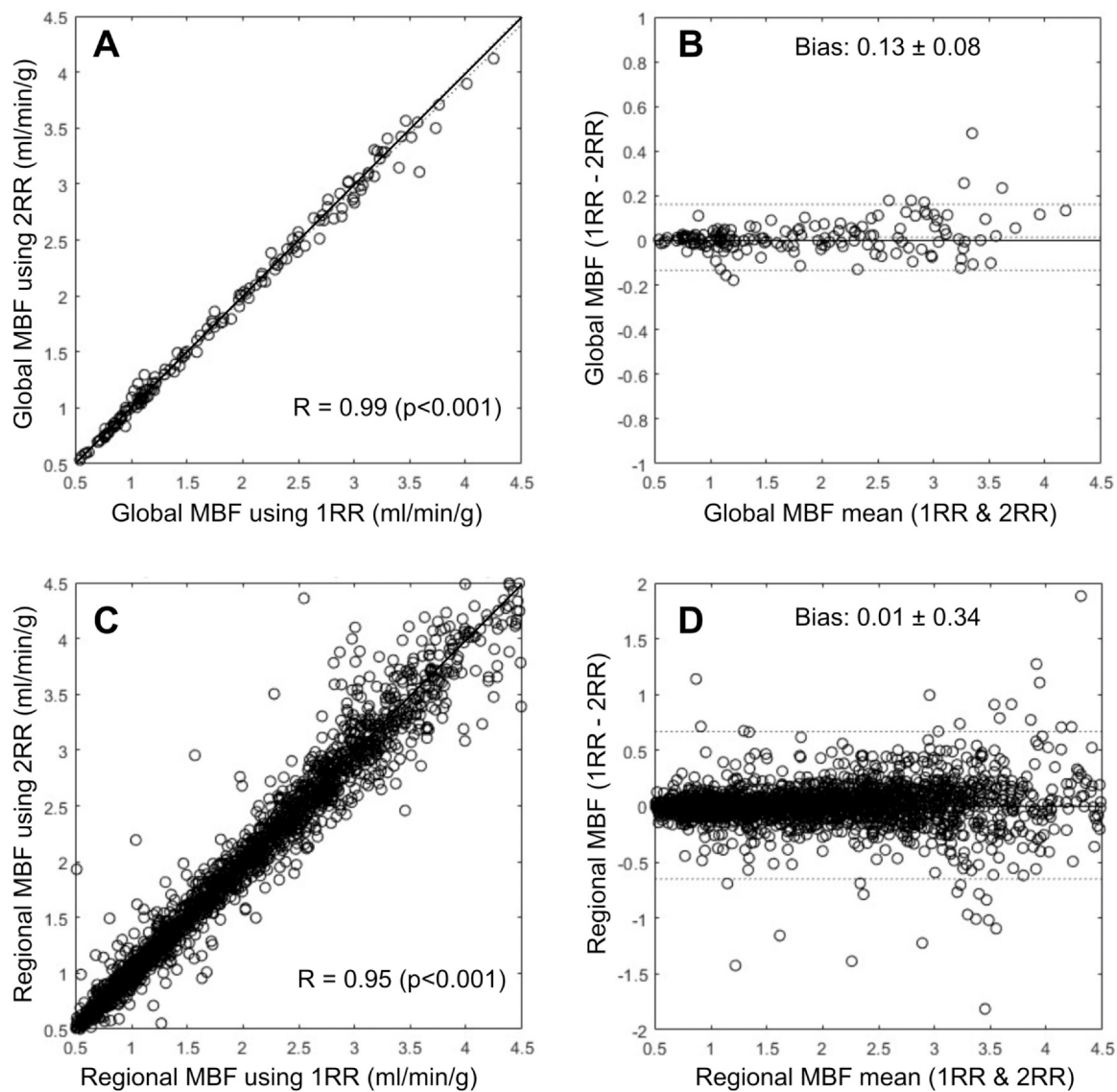


Fig. 3. The agreement between 1RR and 2RR sampling for assessment of global perfusion (rest and stress examinations included). The scatter plots (A, C) and the Bland-Altman plots (B, D) for global perfusion (A, B) and regional perfusion (C, D). There was an excellent agreement and low bias between 1RR and 2RR sampling both for global and regional perfusion. 1RR: sampling every heartbeat; 2RR: sampling every other heartbeat; MBF: myocardial blood flow.

3.2. Diagnostic confidence with 3 vs 6 perfusion maps

Fig. 4 shows the distribution of diagnostic confidence levels with 3 vs 6 perfusion maps, both for 3SAX + 3LAX/2RR (A, B) and for 6SAX/2RR (C, D). There was a significant increase in diagnostic confidence score between all 3 and 6 perfusion maps (1.24 ± 0.68 vs 1.54 ± 0.64 , $p < 0.001$) with similar increase for 3SAX + 3LAX/2RR (1.29 ± 0.68 vs 1.55 ± 0.65 , $p < 0.001$) and for 6SAX/2RR (1.19 ± 0.69 vs 1.53 ± 0.63 , $p < 0.001$). An example, where diagnostic confidence increased by adding 3 LAX is shown in Fig. 5. In 9% (18/204) of the patients, diagnosis changed either from ischemia to no ischemia or vice versa when adding 3 additional perfusion maps. Table 2 shows the distribution of findings from the readings of the 6 perfusion maps (3SAX + 3LAX/2RR or 6SAX/2RR). In 33% (68/204) of the patients, CAD-related ischemia was diagnosed, primarily as single-vessel disease (20%, 40/204). Of the 6 patients with non-CAD ischemia patterns, 5 patients were diagnosed as hypertrophic cardiomyopathy and 1 patient with dilated cardiomyopathy. All 5 patients with hypertrophic cardiomyopathy were found among patients examined by 3SAX + 3LAX/2RR.

The intra- and interobserver variability in diagnostic confidence score were -0.08 ± 0.35 and -0.13 ± 0.61 for 3SAX/2RR only and

-0.10 ± 0.44 and -0.05 ± 0.39 for 3SAX + 3LAX/2RR or 6SAX/2RR, respectively.

3.3. SAX vs LAX perfusion

There was an excellent agreement between SAX and LAX regional perfusion values ($R = 0.97$, $p < 0.001$ with a bias of -0.04 ± 0.27 mL/min/g; Fig. 6) in the subset of 20 patients (a total of 641 SAX-LAX intersections possible to analyze).

3.4. Quantitative perfusion vs findings on invasive angiography

In a total of 50 patients, angiography was performed on clinical indication of which some examples are found in the Appendix. For this subgroup of patients, there was also a significant increase in diagnostic confidence score between 3 and 6 perfusion maps both for 3SAX + 3LAX/2RR (1.31 ± 0.55 vs 1.62 ± 0.57 , $p < 0.001$) and for 6SAX/2RR (1.13 ± 0.74 vs 1.71 ± 0.55 , $p < 0.001$). In 90% (45/50), there was agreement between qFPP and angiography findings. In 23 cases, both qFPP and angiography were positive and in 22 cases qFPP as well as angiography showed normal findings. For the 5 cases with

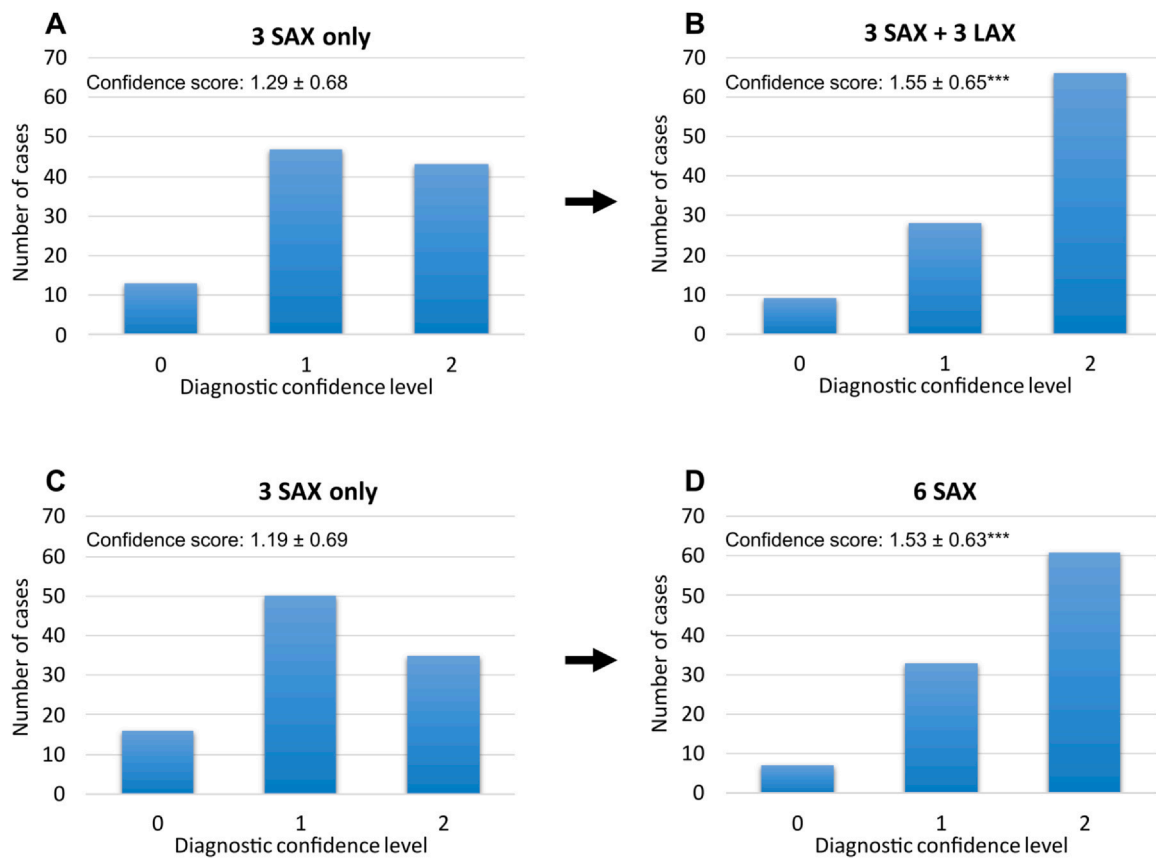


Fig. 4. Diagnostic confidence for ruling in or out stress-induced ischemia when interpreting the results having access to 3 (A, C) or 6 (B, D) perfusion maps, respectively. For both 3SAX + 3LAX (A, B) and for 6 SAX (C, D) the diagnostic confidence increased significantly compared to 3 SAX only. $^{***}p < 0.001$ compared to 3 SAX only. LAX: long-axis view, SAX: short-axis view.

disagreement, qFPP was positive for ischemia with no significant stenosis on angiography. In 1 of the 5 cases, stress-induced ischemia was found in the RCA territory on qFPP, and the RCA showed no stenosis but had an anomalous origin (Appendix Fig. D). In another case, ischemia was detected in LAD and RCA with no significant stenosis on angiography; however, both vessels were described as having variable caliber and spasm tendencies during angiography (Appendix Fig. E). In the remaining 3 cases, qFPP found ischemia in the RCA/LCX territory where no significant stenosis was found on angiography.

4. Discussion

This study shows that diagnostic confidence with single bolus, dual sequence perfusion mapping increases when LV coverage increases from 3 to 6 perfusion maps, either by adding 3 LAX (2-, 3-, and 4-chamber) or 3 SAX views. Furthermore, the study also shows that 1RR and 2RR interval sampling as well as SAX and LAX maps yields comparable perfusion values.

4.1. Sampling every RR interval vs every other (1RR vs 2RR)

Since 2RR sampling showed similar perfusion values as 1RR sampling in the present study, increased LV coverage using this technique is possible without jeopardizing quantitative accuracy. The equivalent values between 1RR and 2RR samplings are in concordance with previously presented preliminary data [22]. Using 2RR sampling results in twice, the number of heartbeats required (120 beats instead of 60) and twice the acquisition time if the number of heartbeats per perfusion map is preserved as was done in the present study. Using additional measurements would theoretically improve the quantification of perfusion over using fewer heart beats since the longer acquisition time

provides more data on the period after the first pass which improves the blood tissue exchange modeling of the interstitial volume. However, the interstitial volume is only weakly correlated with myocardial perfusion and can therefore be considered to have negligible effect on the quantitative perfusion maps. Furthermore, this potential slight improvement by 2RR sampling affects the 3 slices and 6 slices analyzed for diagnostic confidence to the same degree in the present study. The 2RR sampling could, however, be shortened to, i.e., 60 heartbeats (30 heartbeats for 3SAX and 30 heartbeats for 3LAX perfusion maps), which both saves acquisition time and decreases adenosine dose. If the patient has systolic heart failure and low cardiac output, however, a total of 60 heartbeats can be too few to cover the entire first-pass of the contrast bolus, where 120 (and most often 90) heartbeats is sufficient. Since the single bolus, dual sequence perfusion mapping technique [15] used in the present study is executed during free breathing with robust motion correction, prolonging the acquisition does not decrease its clinical utility. Instead, there is a clear advantage with increased LV coverage, especially when heart rate increases above 120 bpm during adenosine stress. With heart rates above 120 bpm, the RR interval becomes too short to allow for acquisition of 3 perfusion views every heartbeat. Thus, 1RR sampling in high heart rates entails that only 2 views of the LV can be acquired and hence incurring a risk of jeopardizing the diagnostic accuracy significantly when all 3 coronary vessel territories are not encompassed. With 2RR sampling, 6 perfusion views are acquired at low heart rate, while 4 views can still be acquired (for example, as 3SAX + 1LAX), when heart rates are above 120 bpm, and thereby ensuring coverage of all coronary vessel territories. Although this is a significant disadvantage when using 3 perfusion views only, no patient in the present study had a heart rate above 120 bpm during stress, indicating that this is rare and less of a clinical problem when using adenosine stress. From experience at our site, heart rate > 120 bpm is

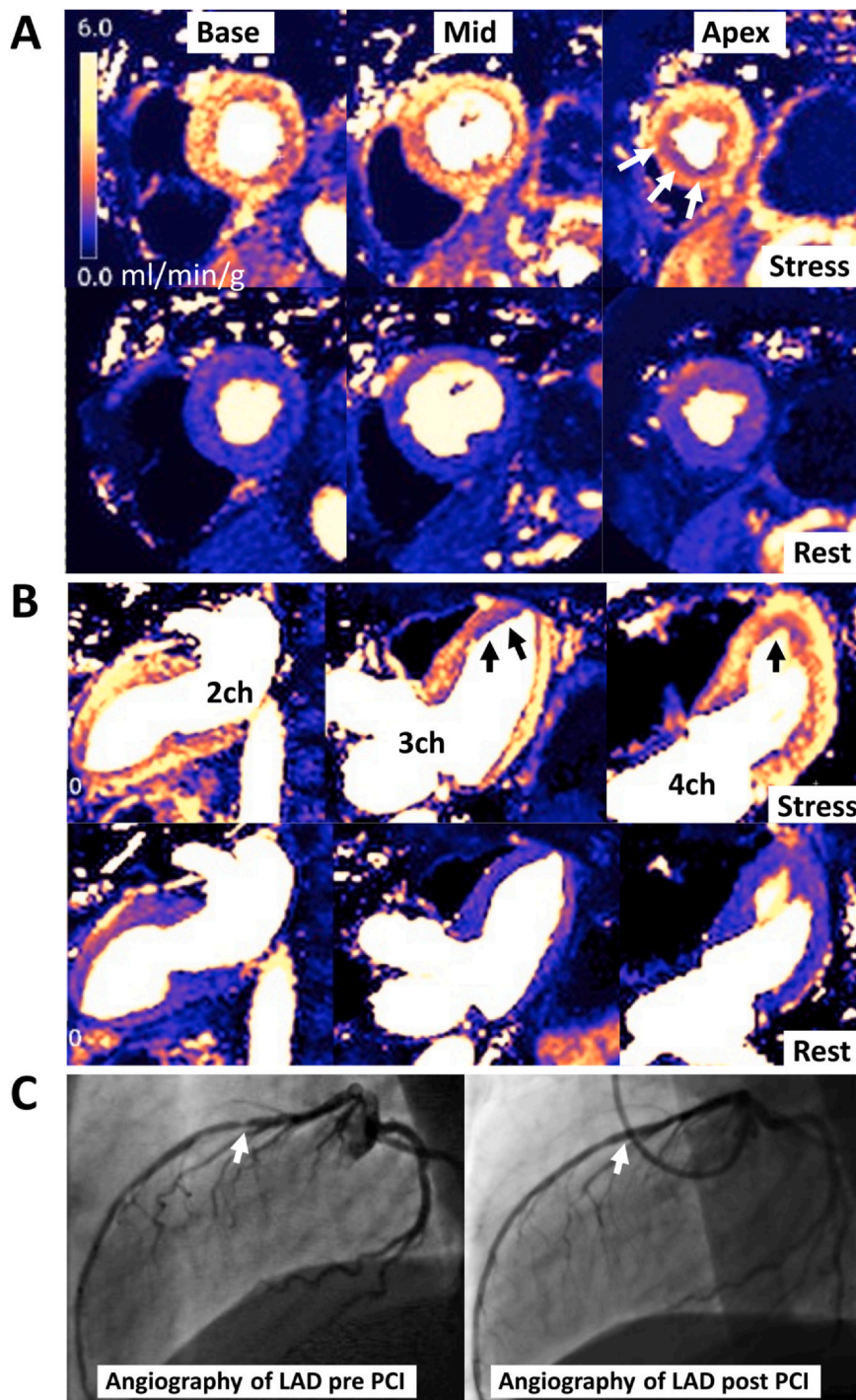


Fig. 5. A case when adding 3 LAX views increases diagnostic confidence. When only having access to the 3 SAX views (3SAX/2RR) (A), the interpretation was *probable ischemia* due to the subendocardial decrease in perfusion in the apical part of septum (white arrows). This changed to *certain ischemia* when including also 3 LAX views (3SAX + 3LAX/2RR) (B) showing decreased perfusion in the 3- and 4-chamber views (black arrows). Angiography (C) showed an LAD stenosis (white arrow) that was successfully revascularized with PCI. LAD: left anterior descending coronary artery, LAX: long-axis view, PCI: percutaneous coronary intervention, SAX: short-axis view.

more often seen when regadenoson is used as stressor, which no patient received in the present study.

The diagnostic confidence increased when adding 3 slices to standard 3 SAX views and the increase was similar regardless of adding 3 additional SAX views or 3 LAX views. Of notice is that all 5 patients where ischemia pattern was suggestive of hypertrophic cardiomyopathy was found using 3SAX + 3LAX/2RR with apical coverage. This is in line with recent findings by Hughes et al. [23] showing that apical coverage by LAX qFPP is important when examining patients with hypertrophic cardiomyopathy, often showing signs of isolated apical perfusion defects.

Applying 2RR sampling to the acquisition provides opportunities for other combinations of perfusion views, such as 5 SAX and 1 LAX (i.e., 2-

chamber view) which is used at some clinical centers. However, which combination of perfusion views that gives the highest diagnostic confidence and accuracy remains to be determined.

4.2. Perfusion imaging vs coronary angiography

We found good agreement between qFPP and angiography with 90% (45/50) of the cases showing congruent findings. A fundamental challenge with assessing the accuracy of perfusion imaging is the inherent lack of a reference standard. There is a large body of literature during the last decades using invasive angiography as reference standard for perfusion imaging. Most often sensitivity, specificity, and predictive values of perfusion imaging are calculated with presence or

Table 2
CMR findings from 3- and 6-slices readings (n = 204).

	3 slices	6 slices
	(3SAX only)	(3SAX + 3LAX or 6SAX)
No ischemia or uncertain	140 (69%)	130 (64%)
CAD-related ischemia	60 (29%)	68 (33%)
Single-vessel disease	34 (17%)	40 (20%)
Multi-vessel disease	12 (6%)	10 (5%)
Microvascular dysfunction	14 (7%)	18 (9%)
Non-CAD related ischemia	4 (2%)	6 (3%)
Splenic switch-off	197 (97%)	197 (97%)

Data expressed as absolute numbers and proportion.

CAD coronary artery disease, LAX long-axis view, SAX short-axis view.

absence of one or more flow-limiting coronary stenoses as ground truth [24]. However, during the recent decades, it has become evident that myocardial perfusion can be affected without flow-limiting coronary stenosis, such as coronary MVD [25] or vasospasm [26,27]. Indeed, one of the patients that showed decreased perfusion in the RCA territory by qFPP with no culprit, flow-limiting stenosis (although variable vessel caliber) showed vasospastic tendency during angiography (Appendix E). Thus, if qFPP should be considered false positive or angiography false negative in this case can be debated and illustrates the challenge with assessing diagnostic accuracy in this context.

In 44% (22/50) of the patients that underwent angiography on clinical indication, both qFPP and angiography were normal or showed non-obstructive coronaries. Thus, these angiographies could potentially have been avoided if qFPP had been performed prior to angiography and used to guide decision to perform angiography or not. These findings are similar to those by Patel et al. [28], showing that 39% of all elective angiographies reveal normal coronary arteries.

4.3. Quantitative first-pass perfusion in relation to other perfusion imaging

Regional perfusion values were found to be similar in SAX and LAX perfusion maps for the same LV segment (Fig. 3) allowing confirmation of findings in 2 orthogonal planes, including apical coverage, to

increase diagnostic confidence. This is exemplified in Fig. 5 where the LAX perfusion maps increased diagnostic confidence of LAD disease. These findings are in line with previously published results by Wang et al. [29] showing benefit of LAX FPP with better coverage of the LV apex. These findings are, however, in contrast with earlier findings by Elkington et al. [30] who were not able to show apical ischemia with LAX FPP echo planar imaging (EPI) in patients with apical ischemia evident by myocardial perfusion single photon emission computed tomography (SPECT). This can potentially be explained by the use of EPI-based FPP compared to SSFP-based imaging used in the present study for qFPP, which has been shown to be superior to EPI [31]. For nuclear myocardial perfusion imaging (myocardial perfusion SPECT and PET), the entire LV myocardium is covered by reconstruction of both SAX and LAX. Thus, conventional FPP imaging with CMR based on 3 short-axis 8 mm LV views (base, midventricular, and apical) has a disadvantage due to limited LV coverage. Previous studies have, however, shown that non-quantitative FPP CMR has similar or superior diagnostic accuracy compared to myocardial perfusion SPECT for diagnosing CAD [32–35]. This might be related to the superior spatial resolution with FPP compared to nuclear imaging. The benefit of higher spatial resolution with CMR compared to myocardial perfusion SPECT has clearly been demonstrated for detection of myocardial infarction where CMR has a higher sensitivity for detection of small and subendocardial infarction compared to myocardial perfusion scintigraphy [36]. Furthermore, qFPP with single bolus, dual sequence using conventional 3 SAX has been shown to have prognostic value in patients with known or suspected CAD [8]. To what extent increased LV coverage and quantitative assessment of perfusion with CMR have added diagnostic and prognostic value remains to be studied.

With the dual-sequence, single-bolus perfusion mapping sequence used in the present study the reader is enabled to retrospectively perform quality checks regarding ECG signal quality, ECG-trigger efficiency, and patient breathing pattern. These are important aspects of diagnostic confidence that are often lacking when interpreting perfusion images acquired by nuclear techniques. Furthermore, FPP also allow for assessment of splenic switch-off as an objective sign of adenosine effect. In 3% (7/204) of the cases in the present study, no splenic switch-off was seen as an indication of insufficient adenosine effect, adding to the number of uncertain cases. These cases would be at risk of being false negative using nuclear imaging where splenic switch-off cannot be assessed.

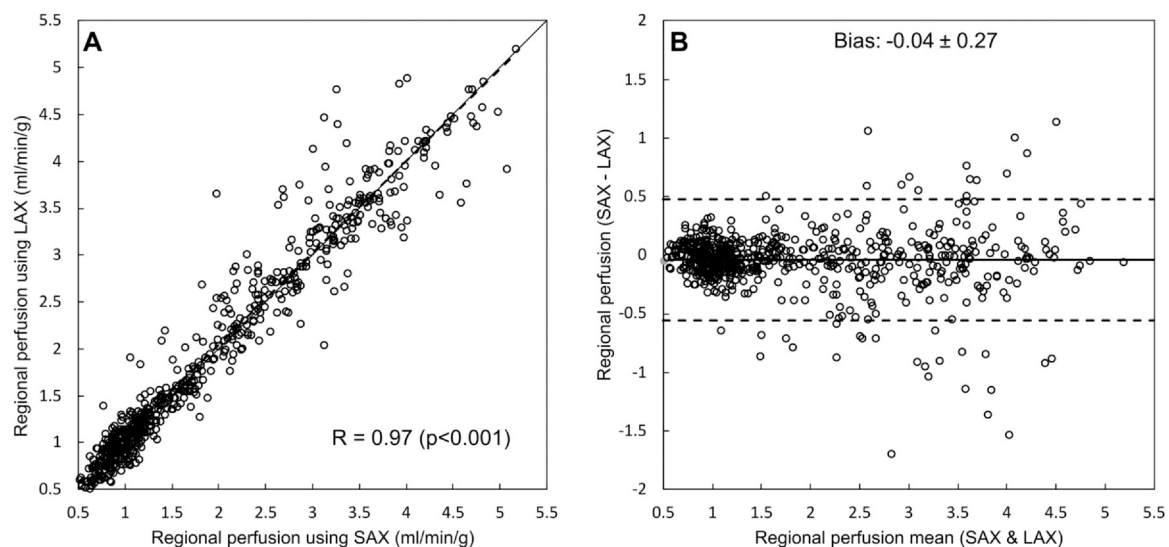


Fig. 6. Agreement between SAX and LAX stress and rest perfusion values from corresponding parts of the left ventricle where the SAX and LAX perfusion maps intersect in a subset of 20 patients (3SAX + 3LAX/2RR). (A) Scatter plot showing a strong correlation between SAX and LAX perfusion values. Solid line represents the line of identity. The Bland-Altman plot (B) shows low bias (-0.04 mL/min/g). Solid line represents the bias, and the dashed lines represents limits of agreement (bias ± 1.96 SD). LAX: long-axis view; SAX: short-axis view.

4.4. Limitations

In the present study, the primary outcome measure of increasing the number of perfusion views from 3 to 6 was diagnostic confidence. As for all clinical studies on myocardial perfusion, the lack of a reference standard constitutes a limitation. Even though angiography cannot be considered reference standard for myocardial perfusion, data from the 50 patients that underwent angiography on clinical indication showed good agreement with qFPP findings. Since most patients with negative findings on qFPP as well as some of the patients with only small areas of ischemia will not undergo angiography, sensitivity, specificity, and predictive values cannot be assessed in this study. Furthermore, for the present study, we have focused on 2 possible combinations of LV views, 3SAX + 3LAX or 6 SAX to assess if increased LV coverage increases diagnostic confidence compared to the conventional 3 SAX. Thus, future studies are required to assess which combination of views that provides most added diagnostic value.

5. Conclusions

Quantitative perfusion mapping of 3 slices with 2RR sampling of data yields similar perfusion values compared to 1RR sampling, allowing for acquisition of additional views within the same perfusion scan. The diagnostic confidence for stress-induced ischemia increases when adding 3 additional views using 2RR sampling, short or long axes, compared to the conventional 3 short-axis views with 2RR sampling. Thus, future development and clinical implementation of quantitative CMR perfusion should aim at increasing the LV coverage from the current standard using 3 short-axis views.

Funding

The work was funded by project grants from Swedish Heart and Lung Foundation and Region of Scania as well as Swedish governmental funding of clinical research (ALF).

Author contributions

Arheden Håkan: Writing – review and editing, Validation, Resources, Methodology, Funding acquisition, Conceptualization. **Kellman Peter:** Writing – review and editing, Methodology, Data curation, Conceptualization. **Xue Hui:** Writing – review and editing, Methodology, Conceptualization. **Aletras Anthony H:** Writing – review and editing, Validation, Methodology, Conceptualization. **Åkesson Julius:** Writing – review and editing, Methodology, Data curation. **Carlsson Marcus:** Writing – review and editing, Methodology, Data curation, Conceptualization. **Ostenfeld Ellen:** Writing – review and editing, Visualization, Methodology, Formal analysis, Conceptualization. **Engblom Henrik:** Writing – review and editing, Writing – original draft, Visualization, Validation, Resources, Project administration, Methodology, Investigation, Funding acquisition, Formal analysis, Data curation, Conceptualization.

Ethics approval and consent

The study was approved by the Lund University Regional ethics committee (dnr 2018/948). All patients gave their written informed consent to participate in the study.

Declaration of competing interest

No declaration of interest for any of the authors.

Acknowledgements

The authors would like to acknowledge the technologists at the Department of Clinical physiology and Nuclear Medicine for their excellent skills and support in acquiring all CMR data.

Appendix A. Supporting information

Supplementary data associated with this article can be found in the online version at [doi:10.1016/j.jocmr.2024.101007](https://doi.org/10.1016/j.jocmr.2024.101007).

References

- [1] Vaduganathan M, Mensah GA, Turco JV, Fuster V, Roth GA. The global burden of cardiovascular diseases and risk: a compass for future health. *J Am Coll Cardiol* 2022;80:2361–71.
- [2] Manning WJ, Atkinson DJ, Grossman W, Paulin S, Edelman RR. First-pass nuclear magnetic resonance imaging studies using gadolinium-DTPA in patients with coronary artery disease. *J Am Coll Cardiol* 1991;18:959–65.
- [3] Schwitzer J, Nanz D, Kneifel S, Bertschinger K, Buchi M, Knusel PR, et al. Assessment of myocardial perfusion in coronary artery disease by magnetic resonance: a comparison with positron emission tomography and coronary angiography. *Circulation* 2001;103:2230–5.
- [4] Atkinson DJ, Burstein D, Edelman RR. First-pass cardiac perfusion: evaluation with ultrafast MR imaging. *Radiology* 1990;174:757–62.
- [5] Wilke N, Jerosch-Herold M, Wang Y, Huang Y, Christensen BV, Stillman AE, et al. Myocardial perfusion reserve: assessment with multisection, quantitative, first-pass MR imaging. *Radiology* 1997;204:373–84.
- [6] Jerosch-Herold M, Wilke N. MR first pass imaging: quantitative assessment of transmural perfusion and collateral flow. *Int J Card Imaging* 1997;13:205–18.
- [7] Mordini FE, Haddad T, Hsu LY, Kellman P, Lowrey TB, Aletras AH, et al. Diagnostic accuracy of stress perfusion CMR in comparison with quantitative coronary angiography: fully quantitative, semiquantitative, and qualitative assessment. *JACC Cardiovasc Imaging* 2014;7:14–22.
- [8] Knott KD, Seraphim A, Augusto JB, Xue H, Chacko L, Aung N, et al. The prognostic significance of quantitative myocardial perfusion: an artificial intelligence-based approach using perfusion mapping. *Circulation* 2020;141:1282–91.
- [9] Knuuti J, Wijns W, Saraste A, Capodanno D, Barbato E, Funck-Brentano C, et al. 2019 ESC Guidelines for the diagnosis and management of chronic coronary syndromes. *Eur Heart J* 2020;41:407–77.
- [10] Zierler KL. Equations for measuring blood flow by external monitoring of radioisotopes. *Circ Res* 1965;16:309–21.
- [11] Axel L. Tissue mean transit time from dynamic computed tomography by a simple deconvolution technique. *Invest Radio* 1983;18:94–9.
- [12] Christian TF, Rettmann DW, Aletras AH, Liao SL, Taylor JL, Balaban RS, et al. Absolute myocardial perfusion in canines measured by using dual-bolus first-pass MR imaging. *Radiology* 2004;232:677–84.
- [13] Gatehouse PD, Elkington AG, Ablitt NA, Yang GZ, Pennell DJ, Firmin DN. Accurate assessment of the arterial input function during high-dose myocardial perfusion cardiovascular magnetic resonance. *J Magn Reson Imaging* 2004;20:39–45.
- [14] Engblom H, Xue H, Akil S, Carlsson M, Hindorf C, Oddstig J, et al. Fully quantitative cardiovascular magnetic resonance myocardial perfusion ready for clinical use: a comparison between cardiovascular magnetic resonance imaging and positron emission tomography. *J Cardiovasc Magn Reson* 2017;19:78.
- [15] Kellman P, Hansen MS, Nielles-Vallespin S, Nickander J, Themudo R, Ugander M, et al. Myocardial perfusion cardiovascular magnetic resonance: optimized dual sequence and reconstruction for quantification. *J Cardiovasc Magn Reson* 2017;19:43.
- [16] Keegan J, Gatehouse PD, Prasad SK, Firmin DN. Improved turbo spin-echo imaging of the heart with motion-tracking. *J Magn Reson Imaging* 2006;24:563–70.
- [17] Cerqueira MD, Weissman NJ, Dilsizian V, Jacobs AK, Kaul S, Laskey WK, et al. Standardized myocardial segmentation and nomenclature for tomographic imaging of the heart: a statement for healthcare professionals from the Cardiac Imaging Committee of the Council on Clinical Cardiology of the American Heart Association. *Circulation* 2002;105:539–42.
- [18] Bergmann SR, Fox KAA, Rand AL, Laskey KD, Welch MJ, Markham J, et al. Quantification of regional myocardial blood-flow in vivo with H₂¹⁵O. *Circulation* 1984;70:724–33.
- [19] Herrero P, Markham J, Shelton ME, Bergmann SR. Implementation and evaluation of a 2-compartment model for quantification of myocardial perfusion with Rb-82 and positron emission tomography. *Circ Res* 1992;70:496–507.
- [20] Xue H, Davies RH, Brown LAE, Knott KD, Kotecha T, Fontana M, et al. Automated inline analysis of myocardial perfusion MRI with deep learning. *Radio Artif Intell* 2020;2:e200009.
- [21] Manisty C, Ripley DP, Herrey AS, Captur G, Wong TC, Petersen SE, et al. Splenic switch-off: a tool to assess stress adequacy in adenosine perfusion cardiac MR imaging. *Radiology* 2015;276:732–40.
- [22] Xue H, Hansen MS, Nielles-Vallespin S, Arai AE, Kellman P. Two RR myocardial perfusion acquisition achieves unbiased myocardial blood flow (MBF) estimates. Abstract presented at: Society for Cardiovascular Magnetic Resonance 2016; 2016; Los Angeles.
- [23] Hughes RK, Augusto JB, Knott K, Davies R, Shiwani H, Seraphim A, et al. Apical ischemia is a universal feature of apical hypertrophic cardiomyopathy. *Circ Cardiovasc Imaging* 2023;16:e014907.
- [24] Takx RA, Blomberg BA, El Aidi H, Habets J, de Jong PA, Nagel E, et al. Diagnostic accuracy of stress myocardial perfusion imaging compared to invasive coronary angiography with fractional flow reserve meta-analysis. *Circ Cardiovasc Imaging* 2015;8.
- [25] Camici PG, d'Amati G, Rimoldi O. Coronary microvascular dysfunction: mechanisms and functional assessment. *Nat Rev Cardiol* 2015;12:48–62.

- [26] Minoda K, Yasue H, Kugiyama K, Okumura K, Motomura K, Shimomura O, et al. Comparison of the distribution of myocardial blood flow between exercise-induced and hyperventilation-induced attacks of coronary spasm: a study with thallium-201 myocardial scintigraphy. *Am Heart J* 1994;127:1474–80.
- [27] Teragawa H, Ueda K, Okuhara K, Kuwashima R, Fukuda Y, Kiguchi M, et al. Coronary vasospasm produces reversible perfusion defects observed during adenosine triphosphate stress myocardial single-photon emission computed tomography. *Clin Cardiol* 2008;31:310–6.
- [28] Patel MR, Peterson ED, Dai D, Brennan JM, Redberg RF, Anderson HV, et al. Low diagnostic yield of elective coronary angiography. *N Engl J Med* 2010;362:886–95.
- [29] Wang Y, Moin K, Mathew ST, Akinboboye O, Reichek N. Myocardial first-pass perfusion assessment using rotational long-axis MRI. *J Magn Reson Imaging* 2005;22:53–8.
- [30] Elkington AG, Gatehouse PD, Prasad SK, Moon JC, Firmin DN, Pennell DJ. Combined long- and short-axis myocardial perfusion cardiovascular magnetic resonance. *J Cardiovasc Magn Reson* 2004;6:811–6.
- [31] Wang Y, Moin K, Akinboboye O, Reichek N. Myocardial first pass perfusion: steady-state free precession versus spoiled gradient echo and segmented echo planar imaging. *Magn Reson Med* 2005;54:1123–9.
- [32] Jaarsma C, Leiner T, Bekkers SC, Crijs HJ, Wildberger JE, Nagel E, et al. Diagnostic performance of noninvasive myocardial perfusion imaging using single-photon emission computed tomography, cardiac magnetic resonance, and positron emission tomography imaging for the detection of obstructive coronary artery disease: a meta-analysis. *J Am Coll Cardiol* 2012;59:1719–28.
- [33] Ahmad IG, Abdulla RK, Klem I, Margulis R, Ivanov A, Mohamed A, et al. Comparison of stress cardiovascular magnetic resonance imaging (CMR) with stress nuclear perfusion for the diagnosis of coronary artery disease. *J Nucl Cardiol* 2016;23:287–97.
- [34] Greenwood JP, Ripley DP, Berry C, McCann GP, Plein S, Bucciarelli-Ducci C, et al. Effect of care guided by cardiovascular magnetic resonance, myocardial perfusion scintigraphy, or NICE guidelines on subsequent unnecessary angiography rates: the CE-MARC 2 randomized clinical trial. *JAMA* 2016;316:1051–60.
- [35] Schwitzer J, Wacker CM, Wilke N, Al-Saadi N, Sauer E, Huettler K, et al. MR-IMPACT II: Magnetic Resonance Imaging for Myocardial Perfusion Assessment in Coronary artery disease Trial: perfusion-cardiac magnetic resonance vs. single-photon emission computed tomography for the detection of coronary artery disease: a comparative multicentre, multivendor trial. *Eur Heart J* 2013;34:775–81.
- [36] Wagner A, Mahrholdt H, Holly TA, Elliott MD, Regenfus M, Parker M, et al. Contrast-enhanced MRI and routine single photon emission computed tomography (SPECT) perfusion imaging for detection of subendocardial myocardial infarcts: an imaging study. *Lancet* 2003;361:374–9.